Mutant Dentin Sialophosphoprotein Causes Dentinogenesis Imperfecta

T. Liang, H. Zhang, Q. Xu, S. Wang, C. Qin, and Y. Lu

Appendix

Supplemental Materials and Methods

Generation of $Dspp^{P19L/+}$ mouse model by CRISPR/Cas9 system

Clustered regularly interspaced short palindromic repeats (CRISPR)/CRISPR-associated protein 9 (Cas9) systems has been widely used to target and modify the endogenous genes in a variety of mammalian cells and organisms (Doudna and Charpentier 2014; Ma et al. 2014). In this study, we employed CRISPR/Cas9 technology to generate $Dspp^{P19L/+}$ knock-in mice. The mouse $Dspp$ gene consists of five exons, and the targeted codon 19 is located in exon 2 (Appendix Fig. 1A). To create a double stranded break targeted to codon 19 of the mouse $Dspp$ gene, a single guide RNA (sgRNA) was designed and synthesized. The guide sequence of the sgRNA consisted of 20 nucleotides (nt) located on the antisense strand directly opposite to codon 19 of the mouse $Dspp$ gene, which was equivalent to codon 17 of the human $DSPP$ gene, and a typical photospacer adjacent motif (PAM) sequence (AGG) was immediately adjacent to its 3' end (Appendix Fig. 1A).

A single-stranded oligodeoxynucleotide (ssODN) of 199 nt was designed, synthesized and used as a template to repair the double stranded break by homology-directed repair. The ssODN repair template contained the centrally located desired pathogenic mutation (CCG>CTG) as well as a silent mutation (GCC>GCG) flanked by two arms of homologous genomic sequence (Appendix Fig. 1A). The pathogenic mutation resulted in the substitution of the proline residue at position 19

of mouse DSPP by a leucine residue (p.P19L). The silent mutation did not change the amino acid sequence of mouse DSPP; instead, it was designed to prevent a successfully edited locus from being further targeted by the sgRNA/Cas9 complex.

A mixture of Cas9 mRNA (100 ng/µL), sgRNA (25 ng/µL) and ssODN repair template (100 ng/µL) was microinjected into the cytoplasm of C57BL6 mouse embryos. The embryos that survived were subsequently implanted into pseudopregnant CD1 female mice. All the mice generated were analyzed for potential $Dspp^{P19L/+}$ or $Dspp^{P19L/P19L}$ founders by polymerase chain reaction (PCR) and DNA sequencing, as described later. The potential founders (F0) were then bred with wild-type C57BL6 mice to obtain F1 mice, which were genotyped to confirm the germline transmission of the desired mutations.

PCR genotyping and DNA sequencing

A combination of PCR, enzymatic digestion, and DNA sequencing was performed to screen for the $Dspp^{P19L/+}$ and $Dspp^{P19L/P19L}$ mice. Genomic DNA was extracted from mouse tail biopsies. The genomic region around the intended mutation site was amplified by PCR using GoTaq Green Master Mix (Promega, Madison, WI) with the following primers, sp276.cel.F (5'-GAGCATGCTGAGGCCCCCACATACC-3') and sp276.cel.R (5'-TGTGTTTGCCTTCATCGAGACCCCA-3'). The PCR program was set as 95 °C for 5 min, followed by 35 cycles of 95 °C for 30 sec, 59 °C for 30 sec, and 72 °C for 45 sec, and a final extension at 72 °C for 7 min. The PCR products were digested with HpaII restriction endonuclease, recognizing the CCGG sequence at the targeted site. The PCR products amplified from wild-type mice were completely cleaved by HpaII into two fragments of 249 bp and 183 bp, whereas the PCR products from the $Dspp^{P19L/+}$ mice were partially digested and the PCR products from the $Dspp^{P19L/P19L}$ mice were completely undigested (Appendix Fig. 1B). DNA sequencing of the PCR

products confirmed that the DSPP mutant mice carried the desired pathogenic mutation at codon 19 (CCG>CTG; p.P19L) and a silent mutation at codon 15 (GCC>GCG; p.A15A) (Appendix Fig. 1C).

Stereo Microscopy

The mandibular molars of 24-week-old $Dspp^{+/+}$ and $Dspp^{P19L/+}$ mice were photographed using a high-precision stereo Olympus SZX16 microscope (Olympus Corporation, Tokyo, Japan).

Plain X-ray radiography and micro-Computed Tomography (µCT)

The left mandibles were dissected from 3-, 8-, and 24-week-old $Dspp^{+/+}$, $Dspp^{P19L/+}$, $Dspp^{P19L/P19L}$ mice, and processed for plain X-ray radiography and µCT analysis, as previously described (Bouxsein et al. 2010; Gibson et al. 2013; Zhang et al. 2018). For three-dimensional (3D) construction and morphometric analyses, an appropriate threshold was determined for each age, based on the visual comparisons. For measuring the dentin thickness, the lowest point at the upper border of the roof dentin concave, and the highest point at the lower border of the floor dentin convex were selected as the reference points. The roof dentin thickness and floor dentin thickness were defined as the thickness of dentin on the line determined by the two reference points on the sagittal plane that transverses the center of the mandibular first molars. The center of the first molar is defined as the sagittal (mesial to distal) section crossing both the most proximal and distal pulp horns, which usually bring two more horns between them, and with the largest apex openings of both proximal and distal root canals selected. All other morphometric parameters were evaluated using the µCT built-in software. It is of note that dentin was analyzed together with cementum as they were indistinguishable by density. The data obtained from 3-5 independent mice for each group were used for the quantitative analysis.

Resin-casted backscattered and acid-etched scanning electron microscopy (SEM)

The 3- and 24-week-old mandible samples were processed for SEM analysis, as described previously (Gibson et al. 2013; Zhang et al. 2018). The samples were dehydrated in gradient ethanol (from 70% to 100%) and xylene before embedded in methyl methacrylate (MMA). The buccal-lingual sections crossing the middle of the proximal root of the mandibular first molar were chosen. The cut surface was polished and dehydrated, followed by gold coating. Scanning was performed in backscattered electronic shadow (BES) mode in a JEOL JSM-6010 LA SEM (JEOL, Japan).

After removal of the coating particles, the sample surface was re-polished and etched with 10% phosphoric acid for 7 seconds for 3-week-old samples and 14 seconds for 24-week-old samples, and soaked in 5% sodium hypochlorite for 20 minutes twice. The samples were then gold-coated and scanned in secondary electron image (SEI) mode in the same SEM.

In situ **hybridization (ISH)**

ISH was performed as previously described (Gibson et al. 2013; Meng et al. 2015; Zhang et al. 2018). Briefly, sections were hybridized with digoxigenin (DIG)-labelled antisense cRNA probes for mouse dentin matrix protein 1 (*Dmp1*) and type I collagen alpha I (*Col1a1*), respectively. After hybridization, the sections were incubated with an anti-digoxigenin antibody conjugated to alkaline phosphatase (1:2000; Roche, Mannheim, Germany), and developed with an NBT/BCIP (nitro blue tetrazolium/5-bromo-4-chloro-3-indolyl-phosphate) substrate (Roche). The sections were counterstained with nuclear fast red (Sigma). At least three individual samples were analyzed for each probe.

Immunohistochemistry (IHC)

IHC was performed to detect DMP1 and phosphorylated Smad1/5/8 using rabbit anti-DMP1

polyclonal antibody (857-3) (Gibson et al. 2013) and rabbit polyclonal anti-p-Smad1/5/8 (pSer463/Ser465) antibody (1:50, Santa Cruz Biotechnology, Inc., Dallas, TX), respectively. The secondary antibody used was biotinylated goat anti-rabbit IgG (H+L) antibody (1:200, Vector Laboratories, Burlingame, CA). The immunostaining signals were visualized using the DAB (3,3'-diaminobenzidine) kit (Vector Laboratories), according to the manufacturer's instructions. The sections were counterstained with methyl green (Sigma).

Extraction of proteins from mouse first molars

Total proteins were extracted from the maxillary and mandibular first molars of the 14-week-old $Dspp^{+/+}$ and $Dspp^{P19L/P19L}$ mice, as described in our previous publications (Qin et al. 2001; Sun et al. 2010). During the extraction procedure, the dental pulp was not separated from the dentin so that the extracted proteins contained DSPP-related proteins from the dental pulp/odontoblasts and predentin as well as the mineralized dentin. The extracted proteins were subject to Western-blotting analysis of DSPP-related proteins, as described below.

Quantitative real-time PCR (qPCR)

Total RNA was extracted from the maxillary and mandibular first and second molars of 3-week-old $Dspp^{+/+}$ and $Dspp^{P19L/+}$ mice using RNeasy Mini Kit (Qiagen, Germantown, MD) and reverse transcribed into cDNA using QuantiTect® reverse transcription kit (Qiagen). qPCR assays were performed using GoTaq® qPCR master mix (Promega, Madison, WI) with a BioRad CFX96 machine (Bio Rad, Hercules, CA). Primer sequences for each gene were provided in Appendix Table 1. Each value was normalized using the value of GAPDH as an internal control. qPCR was done in triplicate for each gene. Four independent mice were analyzed for each genotype.

DNA constructs, cell culture and DNA transfection

Two DSPP-expressing constructs were generated (Appendix Fig. 2A): one expressing a hemagglutinin (HA)-tagged normal mouse DSPP, which was designated as "DSPP-HA"; and the other expressing an HA-tagged mouse mutant DSPP in which the proline residue at position 19 was replaced by a leucine residue [equivalent to the human mutant DSPP (p.P17L)], which we referred to as "P19L-DSPP-HA". The HA tag was inserted after the key cleavage site of DSPP and in the N-terminal portion of DPP. These two constructs were generated by site-directed mutagenesis using the QuikChange site-directed mutagenesis kit (Agilent Technologies, Inc., Santa Clara, CA). The primer sequences used for introducing HA-coding sequnce were forward primer 5'-tgatcccaagagcagcgacgaagttaactacccctacgacgtgcccgactacgcctctaacggaagtgacgaaagtg-3' and reverse primer 5'-cactttcgtcacttccgttagaggcgtagtcgggcacgtcgtaggggtagttaacttcgtcgctgctcttgggatca-3'; the sequence underlined encoded the HA-tag. The primer sequences used for introducing P19L mutation were forward primer 5'-caactgcctgggccattctggttccccagttagtacc-3' and reverse primer 5'-ggtactaactggggaaccagaatggcccaggcagttg-3'. Modifications on the DSPP cDNA sequence were confirmed by DNA sequencing.

HEK 293EBNA (human embryonic kidney 293 Epstein-Barr Virus Nuclear Antigen) cells and 17IIA11 mouse odontoblast-like cells were cultured in Dulbecco's Modified Eagle's Medium (DMEM) supplemented with 10% fetal bovine serum (FBS) as described previously (Lu et al. 2009; Siyam et al. 2012). DNA constructs were transfected into cells using X-tremeGENE™ 9 DNA transfection reagent (Roche, Indianapolis, IN), according to the manufacturer's instructions. For Western-blotting analyses, HEK 293EBNA cells were plated in a 12-well plate at a density of 4×10^5 cells per well; on the next day, the cells were transiently transfected with a total of 1.5 µg of a construct expressing DSPP-HA or P19L-DSPP-HA or an empty vector as a negative control.

Total cell lysates and conditioned media were harvested and analyzed by Western-blotting analysis as described below. For immunofluorescent staining, 17IIA11 cells were plated in a Lab-Tek 4-well slide chamber at a density of 4×10^4 cells per well. On the next day, the cells were transiently transfected with 0.6 µg of a construct expressing DSPP-HA or P19L-DSPP-HA. Twenty-four hours after transfection, the transfected cells were processed for immunofluorescent staining as described below.
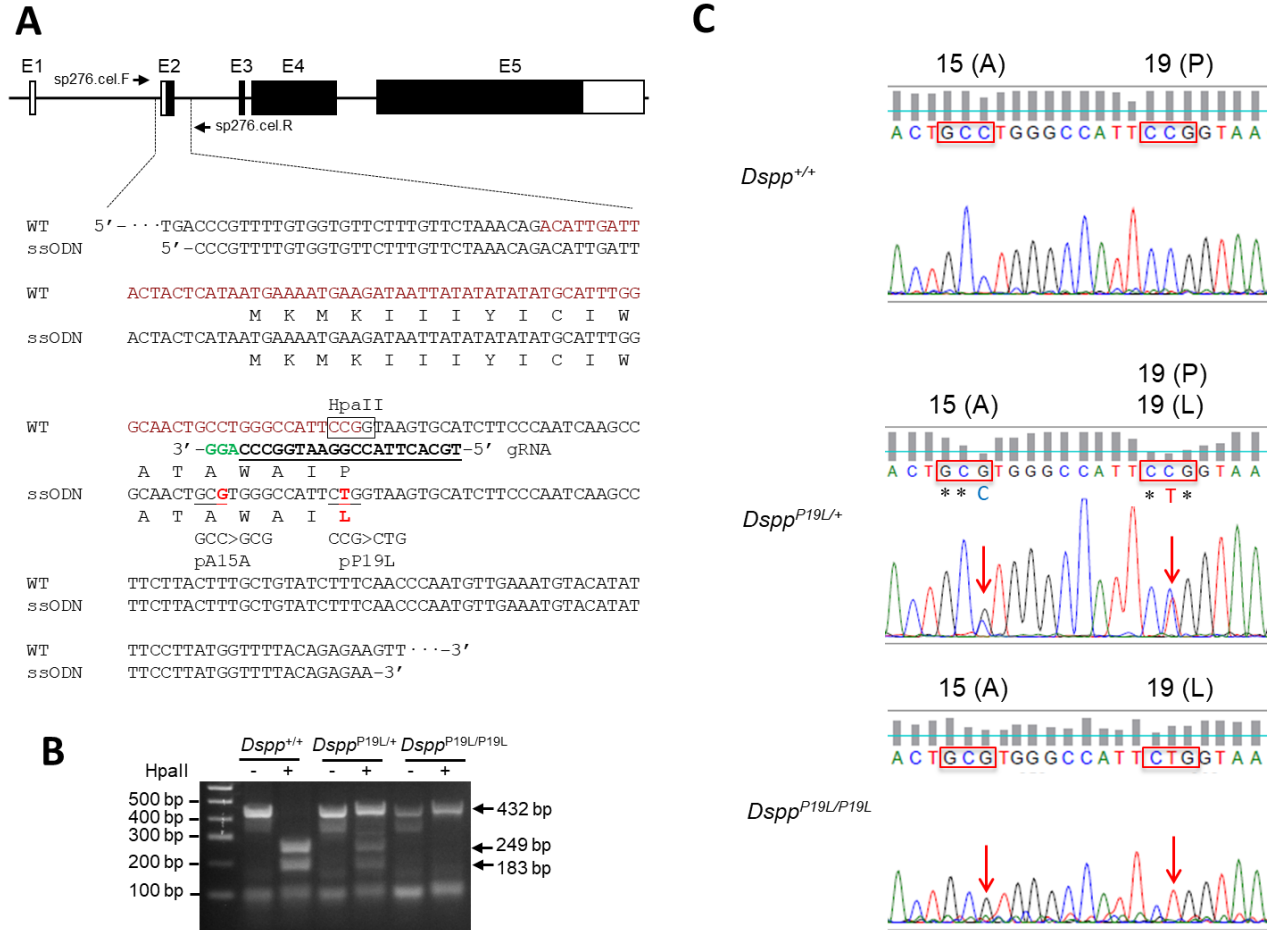
Western-blotting analysis

Western-blotting analysis was performed as previously described (Liang et al. 2016; Sun et al. 2010). Briefly, 40 µg of the total cell lysates, the total proteins extracted with Strataclean resin (Agilent Technologies, Inc.) from 200 µl of conditioned medium or 15 µg of the total proteins extracted from the mouse first molars were electrophoresed on 4-15% gradient SDS-PAGE (sodium dodecyl sulfate-polyacrylamide gel electrophoresis) gels (BioRad, Hercules, CA), and transferred onto a PVDF membrane (EMD Millipore, Billerica, MA). The membranes were blocked in 5% milk (Labscientific, Highlands, NJ), and immunoblotted with mouse monoclonal anti-HA.11 antibody (1:1000, Covance Inc., Dallas, TX) or a rabbit anti-DSP polyclonal antibody (recognizing both DSP and full-length DSPP) at a dilution of 1:4000 (Sun et al. 2010), followed by incubation with HRP-conjugated goat anti-mouse IgG antibody (1:1500; Santa Cruz Biotechnology, Inc., Dallas, TX) or HRP-conjugated goat anti-rabbit IgG antibody (1:2000; Santa Cruz Biotechnology, Inc.). β-actin was immunoblotted with peroxidase-conjugated mouse monoclonal anti-β-actin antibody (1:50000; Sigma). The immunostained protein bands were detected with ECL™ Chemiluminescent detection reagents (Pierce Biotechnology, Inc., Rockford, IL), and imaged by a CL-XPosure film (Pierce Biotechnology).

Immunofluorescent staining

Immunofluorescent staining was performed as described previously (Liang et al. 2016). Briefly, the transfected cells were incubated with mouse anti-HA.11 monoclonal antibody (1:1000; Covance Inc), which targeted HA-tagged DSPP/P19L-DSPP, together with Golgi complex-recognizing rabbit anti-GM130 polyclonal antibody (1:1000; Abcam, Cambridge, MA) or endoplasmic reticulum (ER)-recognizing rabbit anti-calreticulin polyclonal antibody (1:1000; Santa Cruz Biotechnology, Inc.). Fluorescent secondary antibodies used were Alexa Fluor 555 conjugated goat anti-mouse IgG(H+L) (1:1000; Invitrogen) and Alexa Fluor 488 conjugated goat anti-rabbit IgG(H+L) (1:1000; Invitrogen). The nuclei were stained with DAPI. The fluorescent-stained cells were imaged under a Leica DM6000 CFS confocal microscope (Leica Microsystems Inc., Buffalo Grove, IL).

References

Bouxsein ML, Boyd SK, Christiansen BA, Guldberg RE, Jepsen KJ, Muller R. 2010. Guidelines for assessment of bone microstructure in rodents using micro-computed tomography. J Bone Miner Res. 25(7):1468-1486.

Doudna JA, Charpentier E. 2014. Genome editing. The new frontier of genome engineering with crispr-cas9. Science. 346(6213):1258096.

Gibson MP, Zhu Q, Wang S, Liu Q, Liu Y, Wang X, Yuan B, Ruest LB, Feng JQ, D'Souza RN et al. 2013. The rescue of dentin matrix protein 1 (dmp1)-deficient tooth defects by the transgenic expression of dentin sialophosphoprotein (dspp) indicates that dspp is a downstream effector molecule of dmp1 in dentinogenesis. The Journal of Biological Chemistry. 288(10):7204-7214.

Liang T, Meng T, Wang S, Qin C, Lu Y. 2016. The lpv motif is essential for the efficient export of secretory dmp1 from the endoplasmic reticulum. Journal of Cellular Physiology. 231(7):1468-1475.

Lu Y, Qin C, Xie Y, Bonewald LF, Feng JQ. 2009. Studies of the dmp1 57-kda functional domain both in vivo and in vitro. Cells Tissues Organs. 189(1-4):175-185.

Ma Y, Zhang L, Huang X. 2014. Genome modification by crispr/cas9. Febs J. 281(23):5186-5193.

Meng T, Huang Y, Wang S, Zhang H, Dechow PC, Wang X, Qin C, Shi B, D'Souza RN, Lu Y. 2015. Twist1 is essential for tooth morphogenesis and odontoblast differentiation. The Journal of Biological Chemistry. 290(49):29593-29602.

Qin C, Cook RG, Orkiszewski RS, Butler WT. 2001. Identification and characterization of the carboxyl-terminal region of rat dentin sialoprotein. J Biol Chem. 276(2):904-909.

Siyam A, Wang S, Qin C, Mues G, Stevens R, D'Souza RN, Lu Y. 2012. Nuclear localization of dmp1 proteins suggests a role in intracellular signaling. Biochemical and Biophysical Research Communications. 424(3):641-646.

Sun Y, Lu Y, Chen S, Prasad M, Wang X, Zhu Q, Zhang J, Ball H, Feng J, Butler WT et al. 2010. Key proteolytic cleavage site and full-length form of dspp. J Dent Res. 89(5):498-503.

Zhang H, Xie X, Liu P, Liang T, Lu Y, Qin C. 2018. Transgenic expression of dentin phosphoprotein (dpp) partially rescued the dentin defects of dspp-null mice. PLoS One. 13(4):e0195854.

A

E1 sp276.cel.F → E2 E3 E4 E5

← sp276.cel.R

```
WT     5'-···TGACCCGTTTTGTGGTGTTCTTTGTTCTAAACAGACATTGATT
ssODN      5'-CCCGTTTTGTGGTGTTCTTTGTTCTAAACAGACATTGATT

WT     ACTACTCATAATGAAAATGAAGATAATTATATATATATGCATTTGG
              M  K  M  K  I  I  I  Y  I  C  I  W
ssODN  ACTACTCATAATGAAAATGAAGATAATTATATATATATGCATTTGG
              M  K  M  K  I  I  I  Y  I  C  I  W

                            HpaII
WT     GCAACTGCCTGGGCCATTCCGGTAAGTGCATCTTCCCAATCAAGCC
              3'-GGACCCGGTAAGGCCATTCACGT-5'  gRNA
         A  T  A  W  A  I  P
ssODN  GCAACTGCGTGGGCCATTCTGGTAAGTGCATCTTCCCAATCAAGCC
         A  T  A  W  A  I  L
         GCC>GCG      CCG>CTG
         pA15A        pP19L
WT     TTCTTACTTTGCTGTATCTTTCAACCCAATGTTGAAATGTACATAT
ssODN  TTCTTACTTTGCTGTATCTTTCAACCCAATGTTGAAATGTACATAT

WT     TTCCTTATGGTTTTACAGAGAAGTT···-3'
ssODN  TTCCTTATGGTTTTACAGAGAA-3'
```

B

Dspp⁺/⁺ DsppP19L/+ DsppP19L/P19L

HpaII - + - + - +

500 bp
400 bp   ← 432 bp
300 bp
200 bp   ← 249 bp
                          ← 183 bp
100 bp

C

15 (A)   19 (P)

A C T G C C T G G G C C A T T C C G G T A A

Dspp⁺/⁺

19 (P)
15 (A)   19 (L)

A C T G C G T G G G C C A T T C C G G T A A
    * * C   * T *

DsppP19L/+

15 (A)   19 (L)

A C T G C G T G G G C C A T T C T G G T A A

DsppP19L/P19L

Appendix Figure 1. Generation of *DsppP19L/+* knock-in mice. A. Strategy for generating *DsppP19L/+* knock-in mice. Top panel shows a schematic representation of the mouse *Dspp* gene, which consists of 5 exons (E1-E5; white boxes stand for untranslated regions, and black boxes represent coding sequences.). Arrows indicate the locations of the PCR primers, sp276.cel.F and sp276.cel.R, used for genotyping the *DsppP19L/+* knock-in mice. Lower panel shows the sequence of the wild-type (WT) *Dspp* allele, and the corresponding positions of the sgRNA guide sequence (gRNA) and ssODN. The nucleotide sequence of exon 2 is in dark red, and the adjacent sequences

of both introns 1 and 2 are in black. The codon 19 (CCG) is located at the end of exon 2 and encodes a proline residue. The sgRNA guide sequence (bolded and underlined) was designed in close proximity to codon 19 on the antisense strand. The PAM sequence (AGG) is in green. The ssODN was designed to contain the intended nucleotides (in red) for substitution. The deduced amino acid sequences from the WT *Dspp* allele and ssODN are shown below their corresponding nucleotide sequences. The substitution of codon 15 (GCC) by GCG (GCC>GCG) did not cause amino acid change (p.A15A). The substitution of codon 19 (CCG) by CTG (CCG>CTG) led to the substitution of proline residue by leucine residue (p.P19L). The restriction enzyme HpaII recognition site (CCGG) is enclosed in the box. **B.** Genotyping strategy. The *Dspp* alleles were genotyped by PCR using a pair of primers sp276.cel.F and sp276.cel.R., which produced a product of 432 bp. The PCR products were subject to HpaII digestion. The PCR products from the $Dspp^{+/+}$ mice were completely cleaved by HpaII into two fragments of 249 bp and 183 bp. The PCR products from the $Dspp^{P19L/+}$ mice were partially digested and those from the $Dspp^{P19L/P19L}$ mice were completely undigested by HpaII. **C.** DNA sequencing. The *Dspp* alleles were amplified by PCR using sp276.cel.F and sp276.cel.R primers. Shown are the electropherograms of DNA sequencing results of the PCR products from the $Dspp^{+/+}$, $Dspp^{P19L/+}$ and $Dspp^{P19L/P19L}$ mice, respectively. Note the presence of the desired silent mutation (GCC>GCG; p.A15A) and pathogenic substitution mutation (CCG>CTG; p.P19L) in one *Dspp* allele of the $Dspp^{P19L/+}$ mice and in both *Dspp* alleles of the $Dspp^{P19L/P19L}$ mice.
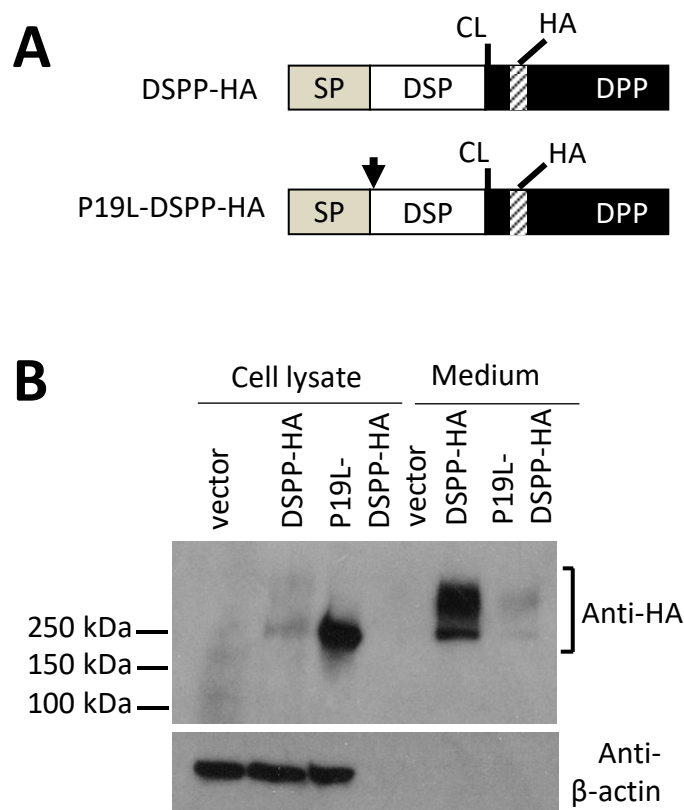
Appendix Figure 2. Intracellular retention of the mouse mutant P19L-DSPP. A. Diagrams of constructs expressing normal mouse DSPP (DSPP-HA) or mutant P19L-DSPP (P19L-DSPP-HA). HA, hemagglutinin tag; CL, key cleavage site of DSPP; SP, ER entry signal peptide; DSP, dentin sialoprotein; DPP, dentin phosphoprotein; the downward arrow indicates the location of the P19L mutation. **B.** Anti-HA Western-blotting analyses of total cell lysates and conditioned medium harvested from HEK 293 EBNA cells transfected with an empty pCDNA3 vector, DSPP-HA or P19L-DSPP-HA construct. β-actin served as loading control for cell lysates. Note that normal DSPP-HA was barely detectable in the cell lysate, but was readily detected in the conditioned medium. In contrast, mutant P19L-DSPP-HA was readily detectable in the cell lysates, but faintly detected in the conditioned medium. Moreover, the secreted P19L-DSPP-HA proteins showed a similar migrating pattern as the normal DSPP-HA proteins on the Western-blot.
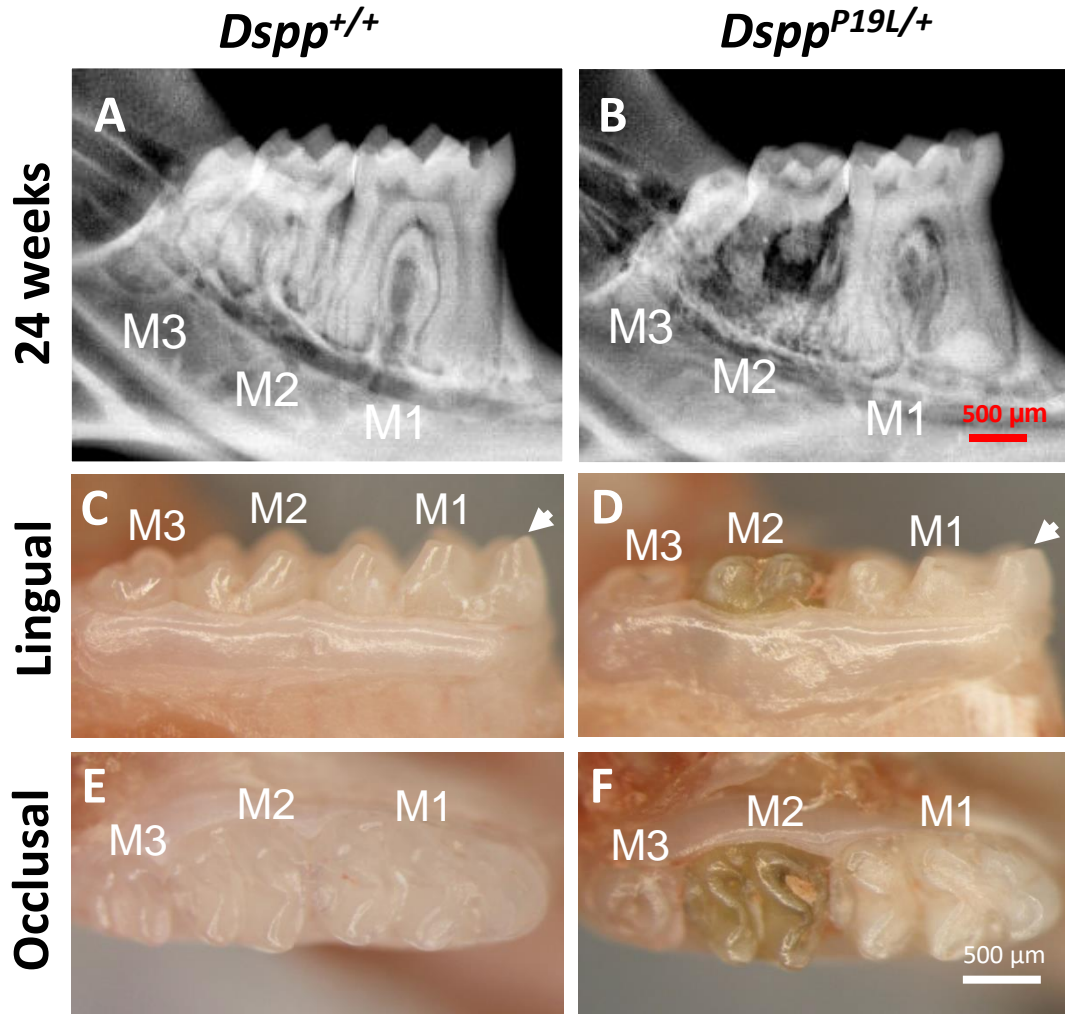
Appendix Figure 3. Plain X-ray radiographic and stereo microscopic analyses of the mandibular molars. A and B. Shown are representative plain X-ray radiographs of the mandibular molars of 24-week-old $Dspp^{+/+}$ (A) and $Dspp^{P19L/+}$ (B) mice. Note the severe destruction of the mandibular second molar (M2) and its surrounding alveolar bone in the $Dspp^{P19L/+}$ mice. **C-F.** Shown are representative photographs of the lingual views (C and D) and occlusal views (E and F) of the mandibular molars of 24-week-old $Dspp^{+/+}$ (C and E) and $Dspp^{P19L/+}$ mice (D and F). The $Dspp^{P19L/+}$ mice showed blunted cusps (arrows) of all molars, and severe discoloration in the mandibular second molars (M2). Abbreviations: M1, first molar; M2, second molar; M3, third molar. Scale bars: 500 µm.
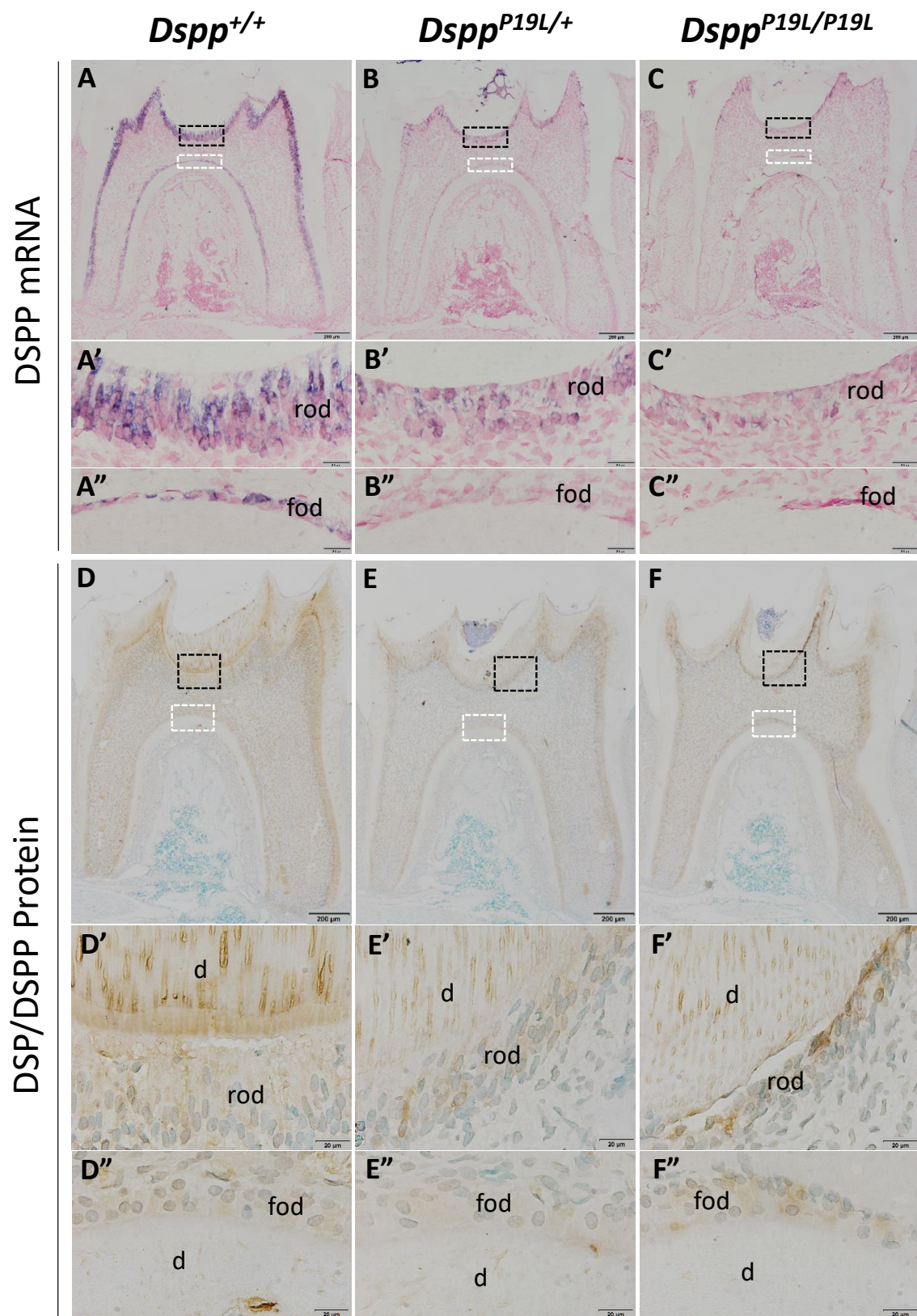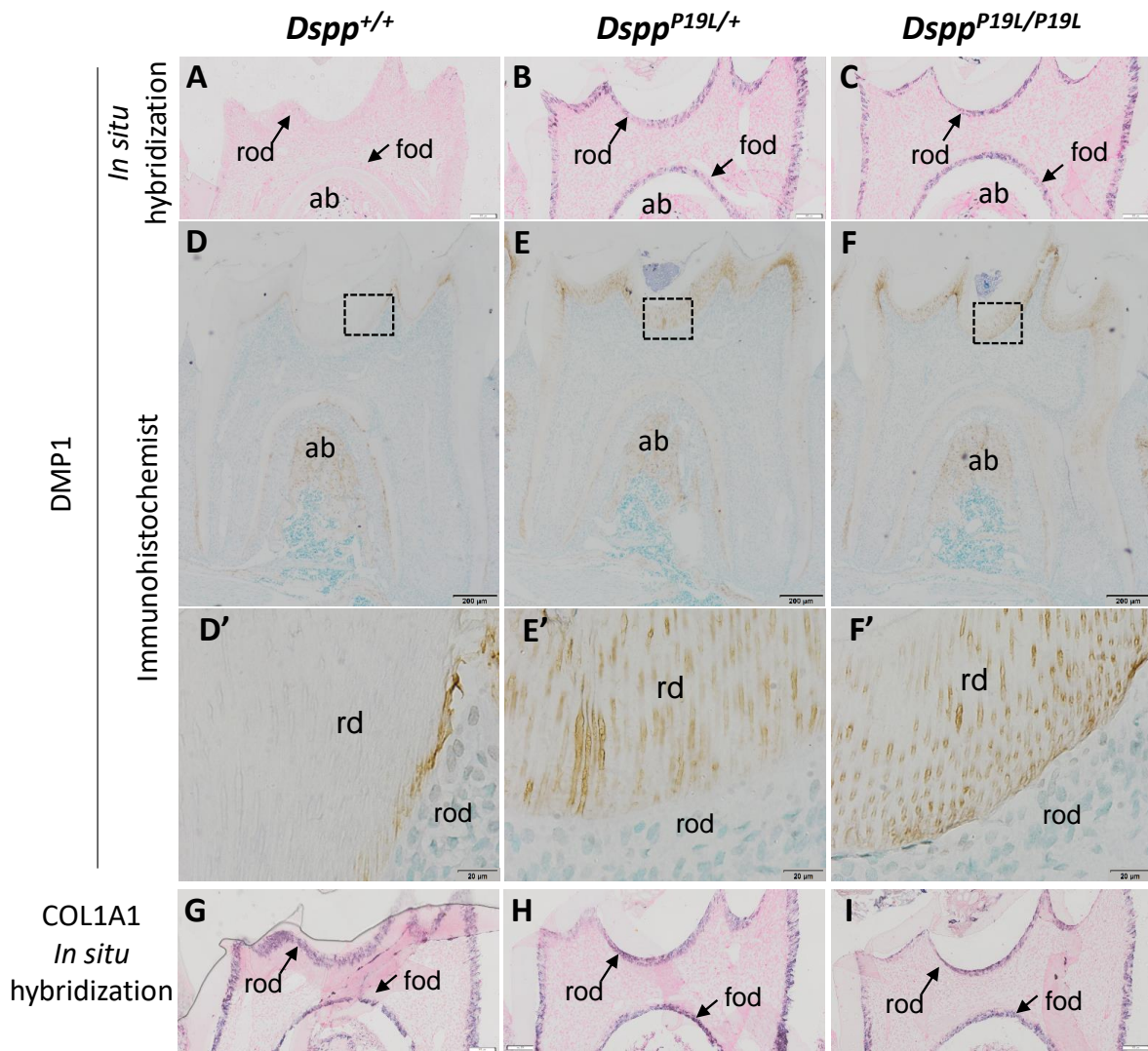
Appendix Figure 4. *In situ* hybridization analyses of DSPP mRNA levels and immunohistochemical

staining of DSP/DSPP protein. Shown are the representative *in situ* hybridization of DSPP mRNA (A-C, signal in purple) and immunohistochemical staining of DSP/DSPP protein (D-F, signal in brown) of the mandibular first molars of 3-week-old *Dspp*$^{+/+}$ (A and D), *Dspp*$^{P19L/+}$ (B and E), and *Dspp*$^{P19L/P19L}$ (C and F) mice. A'-F' are the higher magnification views of the areas marked in black boxes in A-F, respectively. A''-F'' are the higher magnification views of the areas marked in white boxes in A-F, respectively. Abbreviations: d, dentin; rod, roof-forming odontoblast; fod, floor-forming odontoblast. Scale bars: 200 µm in A-F, and 20 µm in A'-F' and A''-F''.
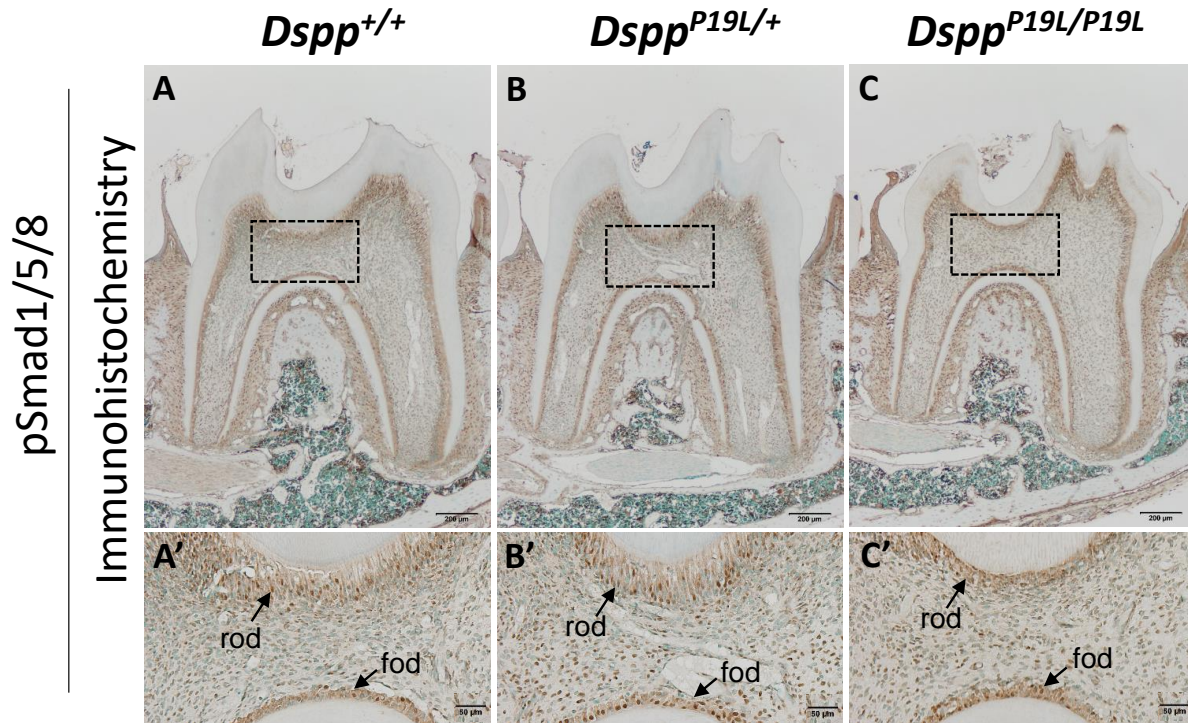
Appendix Figure 5. Immunohistochemical analyses of phosphorylated Smad1/5/8 in the pulp of the mandibular first molars. Shown are the representative immunohistochemical staining results (signal in brown) of phosphorylated Smad1/5/8 (pSmad1/5/8) of the mandibular first molars of 3-week-old $Dspp^{+/+}$ (A), $Dspp^{P19L/+}$ (B), and $Dspp^{P19L/P19L}$ (C) mice. A'-C' are the higher magnification views of the areas marked in black boxes in A-C, respectively. Abbreviations: rod, roof-forming odontoblast; fod, floor-forming odontoblast. Scale bars: 200 µm in A-C and 50 µm in A'-C'.

Appendix Figure 6. Expressions of DMP1 and COL1A1 in the pulp of the mandibular first molars. A-F. Shown are the representative *in situ* hybridization (signal in purple) (A-C) and immunohistochemical staining (signal in brown) results (D-F) of DMP1 in the mandibular first molars of 3-week-old *Dspp*^{+/+} (A and D), *Dspp*^{P19L/+} (B and E), and *Dspp*^{P19L/P19L} (C and F) mice. D'-F' are the higher magnification views of the areas marked in black boxes in D-F, respectively. ISH and IHC analyses showed that DMP1 expression was dramatically increased in the roof-

forming and floor-forming odontoblasts of the $Dspp^{P19L/+}$ and $Dspp^{P19L/P19L}$ mice, compared to the $Dspp^{+/+}$ mice; notably, DMP1 signals in the alveolar bones appeared similar between the DSPP-mutant and wild-type mice. **G-I.** Shown are the representative *in situ* hybridization (signal in purple) results of COL1A1 of the mandibular first molars of 3-week-old $Dspp^{+/+}$ (G), $Dspp^{P19L/+}$ (H), and $Dspp^{P19L/P19L}$ (I) mice. Note that the COL1A1 mRNA levels were similar among the wild-type and DSPP-mutant mice. Abbreviations: rd, roof dentin; rod, roof-forming odontoblast; fod, floor-forming odontoblast; ab, alveolar bone. Scale bars: 200 µm in A-I and 200 µm in D'-F'.

Appendix Table 1. Primers used for qPCR.

Gene	Forward primer	Reverse primer
Dspp	5'-CAGCAAGGATAGCAGTTCTGA-3'	5'-TGTCACTGCCTTCACTGTCAC-3'
Dmp1	5'-AGTGAGTCATCAGAAGAAAGTCAAGC-3'	5'-CTATACTGGCCTCTGTCGTGCC-3'
Col1a1	5'-CTCACGTCCAGATTCACCA-3'	5'-AGAGAGGAGAAAGAGGCTTC-3'
Bsp	5'-GAGACGGCGATAGTTCC-3'	5'-AGTGCCGCTAACTCAA-3'
Oc	5'-CTTGAAGACCGCCTACAAAC-3'	5'-GCTGCTGTGACATCCATAC-3'
Opn	5'-TGATGCCACAGATGAGGACCT-3'	5'-CAGAGGGCATGCTCAGAAGC-3'
Gapdh	5'-CTCCTGGAAGATGGTGATGG-3'	5'-GGCAAAGTGGAGATTGTTGC-3'

Appendix Table 2. Predentin thickness of the mandibular first molars.

	Roof predentin thickness at 1 week (µm)	Roof predentin thickness at 3 weeks (µm)	Floor predentin thickness at 3 weeks (µm)
Dspp$^{+/+}$	10.93±1.07	12.05±1.64	5.63±1.54
Dspp$^{P19L/+}$	10.86±2.28	7.18±1.01a	5.52±0.84
Dspp$^{P19L/P19L}$	10.30±3.00	4.39±1.13ab	5.93±0.30

Notes: n=4; Values are mean ± SD. a: statistically different from *Dspp*$^{+/+}$ (α=0.05). b: statistically different from *Dspp*$^{P19L/+}$ (α=0.05).

Appendix Table 3. qPCR analysis of the expression of the genes encoding odontoblast differentiation markers in 3-week-old mouse molars.

	Dmp1	*Col1a1*	*Bsp*	*Oc*	*Opn*
Dspp$^{+/+}$	1±0.22	1±0.38	1±0.40	1±0.31	1±0.25
Dspp$^{P19L/+}$	5.50±2.22a	0.98±0.33	0.81±0.43	0.77±0.41	0.66±0.56

Notes: n=4; The mRNA levels of *Dspp*$^{+/+}$ mice are set as 1; Values are mean ± SD. a: statistically different from *Dspp*$^{+/+}$ (α=0.05).